Simple chromatic properties of gradient flow

Thomas DeGrand

Simple chromatic properties of gradient flow

Thomas DeGrand[1, *]

[1]*Department of Physics, University of Colorado, Boulder, CO 80309, USA*

Abstract

It has become customary to use a smoothing algorithm called "gradient flow" to fix the lattice spacing in a simulation, through a parameter called t_0. It is shown that in order to keep the length t_0 fixed with respect to mesonic or gluonic observables as the number of colors N_c is varied, the fiducial point for the flow parameter must be scaled nearly linearly in N_c. In simulations with dynamical fermions, the dependence of t_0 on the pseudoscalar meson mass flattens as the number of colors rises, in a way which is consistent with large N_c expectations.

---
[*]Electronic address: `thomas.degrand@colorado.edu`

I. INTRODUCTION

The predictions of lattice studies of systems like QCD are of dimensionless quantities, such as the ratio of two masses. One often wants to present these results as dimensionful numbers (such as masses in GeV). This is done by picking one observable as a fiducial, fixing its value somehow to experiment, and expressing all one's results in terms of it. In lattice QCD simulations, many choices for a scale-setting parameter have been used [1]: masses of various stable particles, decay constants, or quantities derived from the heavy quark potential, such as the string tension or of inflection points in the potential (Sommer parameters [2]). As long as one is studying some system in isolation, there is no deep reason (though there might be practical ones) to favor one choice for a parameter over another. Indeed, the most used quantities for scale setting are arbitrary choices with no direct connection to observation.

There are situations when one might want to compare different theories to each other. The particular comparison, which is the subject of this note, is for systems with different numbers of colors N_c. I am concerned with the N_c dependence of a new fiducial quantity, a squared distance conventionally labeled t_0, which is derived from the diffusive smoothing of the gauge field [3, 4], through a process called "gradient flow" or "Wilson flow." The use of t_0 to set the scale has become standard due to its high accuracy and ease of use. There is a high probability that it will be adopted as a scale setting fiducial for other confining and chirally broken systems. This short paper addresses two questions related to the use of t_0 in such studies:

First, t_0 is a derived quantity; a certain gauge observable, to be defined below, is set to some value which determines t_0. How should that value be set, so that the scale t_0 remains constant with respect to other scales set by gluonic or mesonic observables, as N_c is varied? A simple expectation will be given and tested.

Next, there is a prediction due to Bär and Golterman [5], for the fermion mass dependence of t_0. It comes from a chiral Lagrangian analysis and the small mass limit of their formula involves the pseudoscalar mass m_{PS}, the pseudoscalar decay constant f_{PS} and an undetermined constant k_1,

$$t_0(m_{PS}) = t_0(0)(1 + k_1 \frac{m_{PS}^2}{f_{PS}^2} + \dots) \tag{1}$$

(the full formula is given in Eq. 15, below). Essentially all large scale simulations which measure t_0 observe the linear dependence of t_0 on m_{PS}^2, but with only one value of N_c there is not much one can say about the k_1/f_{PS}^2 part of the expression. Data at several values of N_c reveal that k_1/f_{PS}^2 decreases as N_c rises, in a way which is consistent with large N_c expectations.

In 't Hooft's [6] analysis of QCD in the limit of large number of colors, observables have a characteristic scaling with the number of colors N_c. As in a lattice calculation, the most correct way to express these relations is to talk about dimensionless ratios, though usually this is expressed through statements like "meson masses m_M are independent of N_c, while decay constants scale as $f_{PS} \sim \sqrt{N_c}$." I will use this language in the text. Large N_c expectations, which are well satisfied by lattice data (compare results from pure gauge simulations, summarized in Ref. [7] as well as ones involving fermions from Refs. [8–10]), are that when simulations are performed at the same values of the bare 't Hooft coupling $\lambda = g^2 N_c$, mesonic observables and ones derived from the static potential are approximately independent of N_c, while other observables scale appropriately.

"Gradient flow" or "Wilson flow" is a smoothing method for gauge fields achieved by diffusion in a fictitious (fifth dimensional) time t. In continuum language, a smooth gauge field $B_{t,\mu}$ is defined in terms of the original gauge field A_μ through an iterative process

$$\partial_t B_{t,\mu} = D_{t,\mu} B_{t,\mu\nu}$$
$$B_{t,\mu\nu} = \partial_\mu B_{t,\nu} - \partial_\nu B_{t,\mu} + [B_{t,\mu}, B_{t,\nu}],$$

$$(2)$$

where the smoothed field begins as the original one,

$$B_{0,\mu}(x) = A_\mu(x). \tag{3}$$

Lüscher [3] proposed measuring a distance from flow, using the field strength tensor built using the $B's$, $G_{t,\mu\nu}$, via the observable

$$\langle E(t) \rangle = \frac{1}{4} \langle G_{t,\mu\nu} G_{t,\mu\nu} \rangle. \tag{4}$$

The definition of a squared length t_0 comes from fixing the value of the observable to some value $C(N_c)$

$$t_0^2 \langle E(t_0) \rangle = C(N_c) \tag{5}$$

and treating t_0 as the dependent variable.

Empirically, it is known that at very small t, $t^2 \langle E(t) \rangle$ rises quickly from zero, and then flattens into a linear function of t. The value of $C(N_c)$ which fixes t_0 is chosen to be some value in the linear region.

How does $C(N_c)$ vary with the number of colors, compared to other observables which are expected to be independent of N_c? Lüscher reports that, perturbatively,

$$t^2 \langle E \rangle = \frac{3}{32\pi}(N_c^2 - 1)\alpha(q)[1 + k_1\alpha + ...] \tag{6}$$

where $\alpha(q)$ is the strong coupling constant at momentum scale $q \propto 1/\sqrt{t}$. Using the one-loop formula for the coupling constant,

$$\frac{1}{\alpha(q)} = N_c \frac{B(N_c, N_f)}{2\pi} \log \frac{q}{\Lambda}, \tag{7}$$

where $B(N_c, N_f) = 11/3 - (2/3)N_f/N_c$, we invert Eq. 6 to find

$$\log \frac{q}{\Lambda} = \frac{3}{16} \frac{1}{B(N_c, N_f)C(N_c)}[N_c + O(1) + O(\frac{1}{N_c}) + \ldots]. \tag{8}$$

The scale q is an inverse distance. This expression says that, in order to match distances across N_c, in units of Λ, it must be that $C(N_c) = A_1 N_c + A_0 + ...$ This formula is what I wish to test.

Our scale setting observable is r_1, the shorter version of the Sommer parameter [11]. For ordinary QCD, $r_1 = 0.31$ fm [12]. Its value for the data sets which will be displayed has been previously published in Refs. [8, 10].

II. SIMULATION DETAILS

The data sets are the ones presented in Refs. [10] and [8] plus some additional ones to be described below. The simulations used the Wilson gauge action and clover fermions with normalized hypercubic links [13, 14]. The dynamical fermion simulations had $N_f = 2$ flavors of degenerate mass fermions. All lattice volumes are $16^3 \times 32$. The data sets were approximately matched in lattice spacing, so not much can be said about the size of discretization artifacts. (Note, however, that large N_c comparisons do not necessarily have to be made in the continuum limit.) The spectroscopic data sets were based on about 100 lattices per bare parameter value. (The precise numbers were given in Refs. [8, 10].) Table I records the number of lattices on which flow variables were measured. The lattices from dynamical fermion data sets were typically separated by 10 molecular dynamics time steps; the quenched lattices were separated by 100 Monte Carlo updates using a mixture of over-relaxation and heat bath.

The extraction of t_0 from lattice data is standard. The gradient flow differential equation is integrated numerically using the Runge-Kutta algorithm generalized to $SU(N_c)$ matrices, as originally proposed by Lüscher [3]. The routine discretizes the flow time with a step size ϵ. Calculations used the usual "clover" definition of $E(t)$ [3].

Three aspects of the data need to be described, all of which could influence the results. The first is the choice of integration step size ϵ. To check this, I took one data set (one κ or bare quark mass value) per $SU(N_c)$ and generated an additional data set at a larger step size. Specifically, the data in the tables uses $\epsilon = 0.03$ for $N_c = 2 - 4$ and 0.05 for $N_c = 5 - 7$. I augmented this with an $\epsilon = 0.05$ data set for $N_c = 2 - 4$ and $\epsilon = 0.07$ at $N_c = 5 - 7$. Identical analysis on the two data sets revealed no differences between the results with the two values of ϵ (or more precisely, the differences were about an order of magnitude smaller that the quoted uncertainties).

Next, the dynamical fermion data sets are presumably correlated in molecular dynamics simulation time. I attempted to estimate the autocorrelation time through the autocorrelation function (for a generic observable A) defined as

$$\rho_A(\tau) = \frac{\Gamma_A(\tau)}{\Gamma_A(0)} \tag{9}$$

where

$$\Gamma_A(\tau) = \sum_{i=1}^{N} \left\langle (A(\tau - \bar{A})(A(0) - \bar{A}) \right\rangle . \tag{10}$$

The integrated autocorrelation time (up to a window size W) is

$$\tau_{int}(W) = \frac{1}{2} + \sum_{\tau=1}^{W} \rho(\tau). \tag{11}$$

An issue with these observables is that unless the total length in time of the data set is much larger than the auto-correlation time, it is difficult to estimate an error for them. That is a problem with most of the data sets used; there are typically $O(100)$ measurements. However, it happens that I have additional data for several of the $SU(3)$ and $SU(4)$ sets with about 5000 equilibrated trajectories and 500 saved lattices. I analyzed these sets sets by breaking them into five parts, computing τ_A on each part, and taking an error from the part-to-part fluctuations.
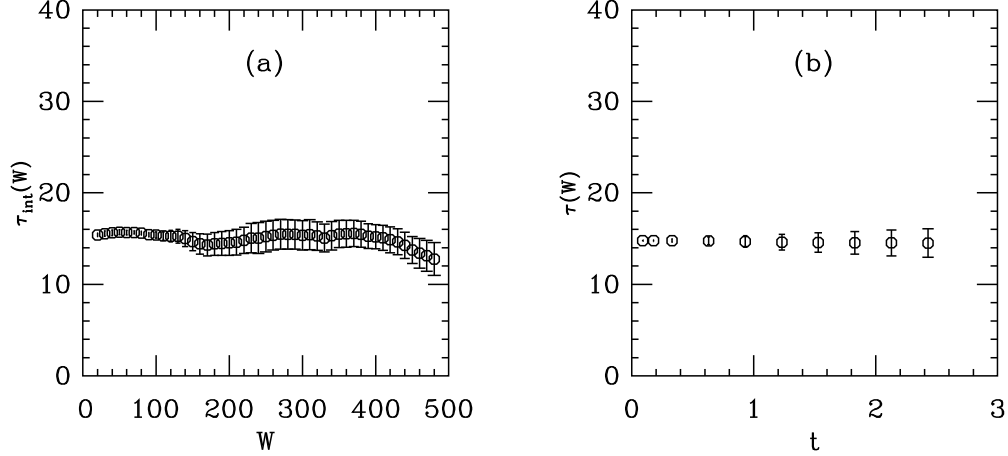
4

FIG. 1: Integrated auto-correlation times for an $SU(4)$ data set, $\beta = 10.2$, $\kappa = 0.127$. (a) $\tau_{int}(W)$ vs W in molecular dynamics time units, at flow time $t = 2.0$. (b) $\tau_{int}(W)$ for $W = 20$ lattices (or $W = 200$ molecular dynamics time units) for a set of flow values t.

All of these data sets produce similar results. I show pictures from one data set, an $SU(4)$ gauge group with $\beta = 10.2$, $\kappa = 0.127$. Panel (a) of Fig. 1 shows the integrated auto-correlation time for $t^2 E(t)$ as a function of W, measured in molecular dynamics time units (rescaled from data sets spaced ten molecular dynamics units apart). Panel (b) shows $\tau_{int}(W = 200)$ for a scan of flow time values. With a spacing of 10 molecular dynamics units between saved lattices, if an auto-correlation time were less than 10 molecular dynamics units, it would be hard to observe.

Finally, there is the determination of t_0 (or of $C(N_c)$ itself). Here the issue is that on each lattice, data at all values of flow times t are correlated simply because later flow time data are constructed by processing earlier flow time data. I dealt with this by doing a jackknife analysis, basically along the lines of the ones done by Ref. [15]. The analysis displayed in Fig. 1 suggests doing the jackknife eliminating sets of lattices whose length is longer than the integrated auto-correlation time. This is two successive lattices for $\tau_{int} = 20$ molecular dynamics time units. I varied the size of the cut; even eliminating 10 successive lattices from the jackknife (100 molecular dynamics time units) generally resulted in only a 20 per cent rise in the quoted uncertainty.

Two sets of numbers are needed, values of $C(N_c)$ at a fixed ratio of t_0/r_1^2, and values of t_0 at an input $C(N_c)$. These values are determined by a fit to a small set of points roughly centered around the fit value to a linear dependence ($t^2 \langle E(t) \rangle = c_0 + c_1 t$) followed by a linear interpolation to the desired value. These results were collected and the jackknife produced the numbers quoted in the table. I varied the range of the fit and the number of points kept; as long as the central values lie within the range of points kept, their values are insensitive to the fit range.

III. RESULTS

A. $C(N_c)$ vs N_c

Lüscher suggested taking $C(N_c) = 0.3$ for $N_c = 3$ QCD. The resulting t_0 has been evaluated by many groups[15–20], $\sqrt{t_0} = 0.14$ fm in $N_f = 3$ QCD. (The quantity is actually known to four digits.) Let us keep the ratio $\sqrt{t_0}/r_1$ fixed, $\sqrt{t_0}/r_1 = 0.46$, while varying N_c, and ask how $C(N_c)$ is changed. Fig. 2 shows data from quenched $SU(N_c)$ simulations with $N_c = 3, 5, 7$ [8], and data from $N_f = 2$ dynamical fermion simulations with $N_c = 2, 3, 4,$ 5 [10]. (Error bars in the figure are dominantly from the uncertainty in r_1.) The data are tabulated in Table II. The dynamical fermion data are at roughly constant pseudoscalar to vector mass ratio, so they are matched in fermion mass. The gauge couplings and fermion hopping parameters are $(\beta, \kappa) = (1.9, 0.1295), (5.4, 0.127), (10.2, 0.1265)$ and $(16.4, 0.1265)$, for $N_c = 2, 3, 4,$ and 5, from the data sets of Ref. [10]. $C(N_c)$ clearly varies linearly with N_c. It is not a pure linear dependence; $C(N_c) = A_1 N_c + A_0 + ...$ and the A_0 and higher order contributions are due to $1/N_c$ corrections canceling the leading N_c dependence in Eq. 8. Presumably, the higher order corrections are also N_f dependent.

I have not found a fit with a chi-squared per degree of freedom which is near unity. The figure shows a one attempt: I fit all the data (quenched and $N_f = 2$ to

$$C(N_c, N_f) = c_1 N_c + c_2 N_f + \frac{c_3}{N_c} + c_4. \tag{12}$$

The fit has a χ^2 of 11.6 for 3 degrees of freedom; $c_1 = 0.096(3)$, $c_2 = 0.014(2)$, $c_3 = 0.0267(46)$, $c_4 = -0.093(26)$.

Finally, the authors of Ref. [21] use

$$C(N_c) = 0.3 \left(\frac{3}{8} \frac{N_c^2 - 1}{N_c} \right) \tag{13}$$

to match scales in their quenched calculation of the topological susceptibility. This absorbs all the leading factors of N_c in the quenched versions of Eqs. 6-7 (or, said alternatively, makes an all-orders ansatz for its N_c counting), while fixing the $N_c = 3$ value to $C(3) = 0.3$. This seems to over-estimate the slope of $C(N_c)$ versus N_c, when compared to r_1, for the $N_f = 2$ data sets. It would give $C(N_c = 7) = 0.77$.

I conclude this section by remarking that matching $C(N_c)$ by taking one value of t/r_1^2 to be an N_c independent constant produces a match of lattice data at different N_c's across a wide range of t. This is displayed in Fig. 3.

B. t_0 vs m_{PS}^2

I next fix the value of $C(N_c)$ and collect data at many values of the quark mass, using the data sets of Ref. [10]. I evaluate t_0 using the values of $t^2 \langle E(t) \rangle$ which match length scales, as shown in Fig. 2. They are $C(N_c) = 0.26, 0.3, 0.38,$ and 0.47 for $N_c = 2, 3, 4,$ and 5. The data is tabulated in Table I. With this data, I ask, can we observe the fermion mass dependence of t_0 predicted by the chiral Lagrangian analysis of Bär and Golterman [5]? They write an expansion for $E(t)$ in terms of the characteristic length scale for a chiral Lagrangian,

$$E(t) = c_1 f_{PS}^4 + \cdots + c_3 f_{PS}^2 \text{Tr} \left(\chi^\dagger U + U^\dagger \chi \right) + \ldots \tag{14}$$
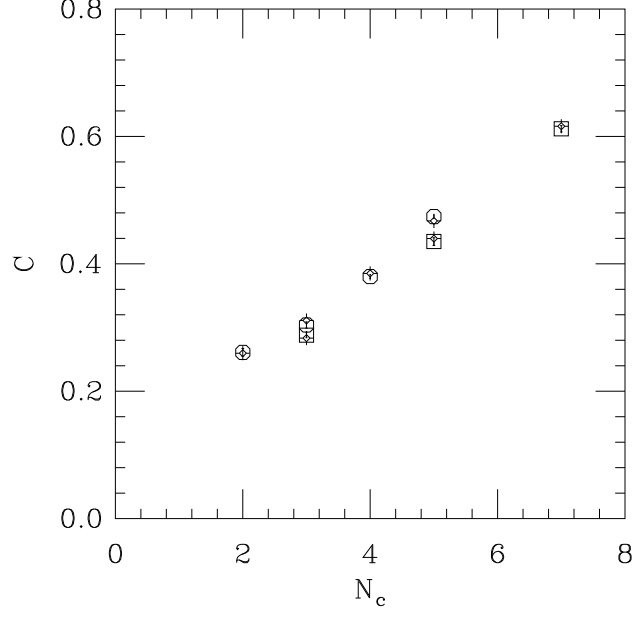
FIG. 2: Tuning factor $C(N_c)$ from 5, matching $\sqrt{t_0}/r_1 = 0.46$. Octagons are dynamical fermion data while squares are quenched. The fancy diamonds are a fit to both data sets described in the text.
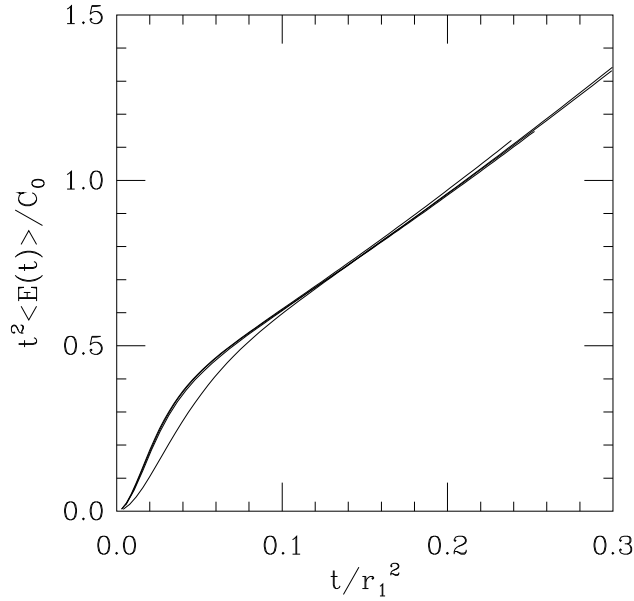

FIG. 3: Plots of $t^2 \langle E(t) \rangle$ scaled by N_c-dependent constants, as a function of t/r_1^2. The data sets and constants are: (SU(2): $\beta = 1.9$, $\kappa = 0.1295$, $C_0 = 0.26$); (SU(3): $\beta = 5.4$, $\kappa = 0.127$, $C_0 = 0.3$); (SU(4): $\beta = 10.2$, $\kappa = 0.1265$, $C_0 = 0.38$); (SU(5): $\beta = 16.4$, $\kappa = 0.1265$, $C_0 = 0.47$). The $SU(2)$ curve is the slightly discrepant one at small t.

where f_{PS} is the pseudoscalar decay constant, U is the usual exponential of the Goldstone boson field, χ is proportional to the fermion mass or to the squared pseudoscalar mass m_{PS}^2, and the c_i's are a set of dimensionless coefficients. They then predict

$$t_0(m_{PS}) = t_0(0)(1 + k_1\frac{m_{PS}^2}{f_{PS}^2} + k_2\frac{m_{PS}^4}{f_{PS}^4}\log(\frac{m_{PS}^2}{\mu^2}) + k_3(\frac{m_{PS}^2}{f_{PS}^2})^2 + \ldots) \qquad (15)$$

where $t_0(0)$ is the value of the flow parameter at zero mass, The k_i's are also dimensionless constants, ratios of the c_i's. Judging from the quality of the data in Ref. [10], it should be possible to observe the leading (proportional to k_1) mass dependence in this expression. The result is shown in Fig. 4. There is a definite, more or less linear, dependence of t_0 on the squared mass, for all N_c's. The slope flattens as N_c rises.

The flattening of the slope follows the naive expectation that fermions affect gauge observables less and less as N_c rises. It also tells us a bit more. In Eqs. 14 and 15 the constants c_i and k_i are dimensionless, but of course this does not say anything about how the higher order terms c_3 or k_1 scale with N_c.

Data from several N_c's allows us to say something about k_1. The pseudoscalar decay constant scales as $\sqrt{N_c}$. How does k_1 depend on N_c? We can look at that behavior by rescaling the data. Eq. 15 can be rewritten as

$$\frac{t_0(m_{PS})}{t_0(0)} - 1 = \frac{k_1}{f_{PS}^2}m_{PS}^2 + \ldots. \qquad (16)$$

I observe that k_1/f_{PS}^2 scales like $1/N_c$. To see if that expectation holds, plot the scaled quantity $N_c(t_0(m_{PS})/t_0(0) - 1)$ versus m_{PS}^2 and look for a common slope.

Fig. 5 shows this. Bär and Golterman say that their formula is applicable for flow times much smaller than the square of the pion wavelength. With $t_0 \sim 2 - 2.5a^2$ it seems appropriate to concentrate on $(am_{PS})^2 < 0.2$ or so, and that is what is shown in the figure. The intercept t_0 is determined by doing a quadratic fit of $t_0(m_{PS})$, $t_0(m_{PS}) = t_0(0) + A(am_{PS})^2 + B(am_{PS})^4$. The plot uses $t_0(0) = 2.27$, 2.71, 2.62, 2.36 and 2.17 for $SU(2)$ $\beta = 1,9$, $SU(2)$ $\beta = 1.95$, $SU(3)$, $SU(4)$, and $SU(5)$. Data for different $N_c \geq 3$ seems to behave similarly – a linear dependence on m_{PS}^2 with an N_c - independent slope. This says that k_1 is a constant, independent of N_c. (Linear fits to the points shown in the figure give slopes $N_c k_1/f_{PS}^2 = -3.7(2)$ and -3.1(2) for the $\beta = 1.9$ and 1.95 $SU(2)$ points, -4.3(1) for $SU(3)$, -4.4(2) for $SU(4)$, and -3.9(2) for $SU(5)$.)

This result has a more mundane large N_c origin. $E(t)$ is dominantly a gluonic observable, $\langle E(t)\rangle \propto \langle g^2 G^2)\rangle$ (re-inserting a factor of g^2 as compared to Eq. 4). $\langle G^2\rangle$ is also a gluonic observable, which scales as N_c^2. (Think of it as a closed gluon loop.) The coupling scales as $g^2 = \lambda/N_c$ for 't Hooft coupling λ. Thus, $\langle E(t)\rangle \propto N_c$ at fixed λ. This is the scaling for $C(N_c)$ seen in Fig. 2. Because f_{PS} scales as $\sqrt{N_c}$, c_1 in Eq. 14 must scale as $1/N_c$, and then $c_1 f_{PS}^4 \propto N_c$. The second term in Eq. 14 is a fermionic contribution to a gluonic observable, which is a $1/N_c$ effect: that is, $(c_3 f_{PS}^2)/(c_1 f_{PS}^4) \propto 1/N_c$, or $k_1 = c_3/c_1 \propto N_c^0$. (Think of breaking the gluon loop into a $q\bar{q}$ pair: this costs a factor of g^2 while leaving the double-line color counting N_c^2 unchanged. Replacing g^2 by λ/N_c gives a $1/N_c$ suppression.) This is what Fig. 5 shows.

Note that the only parts of Eq. 15 which are unambiguously "fermionic" rather than "gluonic," and which are accessible to simulation, are the terms with explicit quark mass (or m_{PS}) dependence.
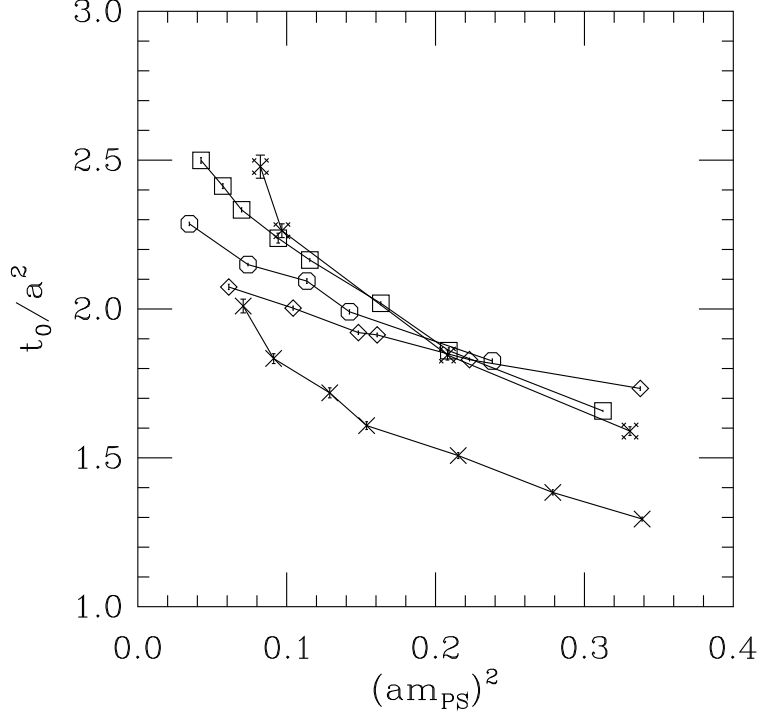
8

FIG. 4: The quantity t_0/a^2 versus squared pseudoscalar mass in lattice units, $(am_{PS})^2$, for $N_c = 2$ (crosses for $\beta = 1.9$, fancy crosses for $\beta = 1.95$), 3 (squares), 4 (octagons), and 5 (diamonds).

We would expect $N_c = 2$ to be an outlier. The pattern of chiral symmetry breaking is different for $SU(2)$ than for $N_c \geq 3$ since the fermions live in pseudo-real representations. Generally, that means that the coefficients in a chiral expansion are different from the usual factors appropriate to complex representations. Nevertheless, the plots of t_0 versus mass show empirically that the value of k_1 does not seem to be very different.

IV. CONCLUSIONS

In this note I discussed the N_c dependence of the flow scale t_0 and compared it to simple theoretical expectations. I observed that in order to match the t_0 scale to that of other gluonic observables it was necessary to scale $t^2 \langle E(t) \rangle$ in a particular way with N_c. (I used the Sommer parameter r_1, derived from the heavy quark potential.) I also observed the decoupling of t_0, a gluonic observable, from fermionic degrees of freedom, as N_c grows. Measurements of $t_0(m_{PS}^2)$ at several values of N_c are the closest one can come to observing the $1/f_{PS}^2$ in the Bär-Golterman formula.

In QCD, the flow time t_0 is presently the quantity of choice for scale setting, and one would expect that it would find use in simulations of other confining and chirally broken systems. Researchers who use it will discover that the dependence of $t^2 \langle E(t) \rangle$ on t will be different for their system than for $N_c = 3$ QCD. An analysis similar to the one described here might allow them to justify some particular choice for C. A useful part of the analysis of any new model is to ask "how is it different from real world QCD?" Part of the answer to this question involves the analysis of Monte Carlo data, and a scale choice is a necessary
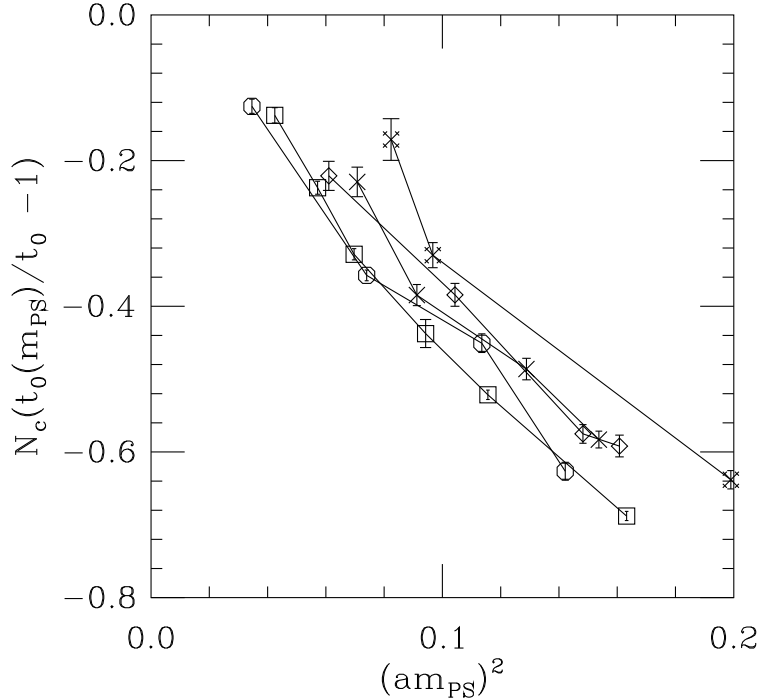
FIG. 5: The shifted quantity $N_c(t_0(m_{PS})/t_0 - 1)$, versus squared pseudoscalar mass in lattice units, $(am_{PS})^2$, for $N_c = 2$ (crosses for $\beta = 1.9$, fancy crosses for $\beta = 1.95$), 3 (squares), 4 (octagons), and 5 (diamonds).

part of this analysis. A comparison of a new system with QCD might involve matching the scale choice used for the new system with the one used for QCD, which would require an analysis similar to the one done here.

In addition, there is more to the analysis of a new system than Monte Carlo data. It is often useful to have a model, which can hint at results which have not yet been computed on the lattice, or which may not be accessible to the lattice. (Large N_c counting is an example of such a model.) However, models typically are incomplete. Some observed behavior might have a simple and unexpected source (given by large N_c counting, for example), but it may not be something which can be completely justified from first principles. It is always useful to verify and confirm assumptions and common lore, in a sound and reliable way.

Acknowledgments

κ	$(a\,m_{PS})^2$	t_0/a^2	N
$SU(2)$ $\beta = 1.9$	$C = 0.26$		
0.1280	0.339(2)	1.295(7)	40
0.1285	0.279(3)	1.384(9)	40
0.1290	0.215(3)	1.508(10)	40
0.1295	0.154(3)	1.608(13)	40
0.1297	0.129(2)	1.718(17)	40
0.1300	0.091(3)	1.833(16)	40
0.1302	0.071(3)	2.010(23)	40
$SU(2)$ $\beta = 1.95$	$C = 0.26$		
0.1270	0.331(3)	1.590(15)	40
0.1280	0.208(2)	1.845(17)	40
0.1290	0.097(2)	2.263(23)	40
0.1292	0.082(2)	2.478(39)	40
$SU(3)$ $\beta = 5.4$	$C = 0.3$		
0.1250	0.312(2)	1.657(3)	500
0.1260	0.209(1)	1.860(10)	100
0.1265	0.163(2)	2.019(6)	500
0.1270	0.116(2)	2.165(6)	500
0.1272	0.094(2)	2.238(17)	100
0.1274	0.070(2)	2.333(7)	500
0.1276	0.057(1)	2.413(8)	500
0.1278	0.042(1)	2.500(9)	500
$SU(4)$ $\beta = 10.2$	$C = 0.38$		
0.1252	0.238(2)	1.826(7)	90
0.1262	0.142(1)	1.990(7)	90
0.1265	0.114(1)	2.094(8)	100
0.1270	0.074(1)	2.149(4)	500
0.1275	0.035(1)	2.286(6)	500
$SU(5)$ $\beta = 16.4$	$C = 0.47$		
0.1240	0.338(1)	1.733(5)	90
0.1252	0.223(1)	1.830(5)	90
0.1258	0.161(2)	1.913(6)	90
0.1260	0.148(1)	1.920(6)	90
0.1265	0.104(1)	2.003(7)	90
0.1270	0.061(1)	2.074(9)	90

TABLE I: $N_f = 2$ dynamical fermion data plotted in the figures. The column labeled by N gives the number of lattice analyzed for t_0. The data is that of Ref. [10]. Pseudoscalar masses are reproduced for convenience.

N_c	β	κ	$C(N_c)$
3(Q)	6.0175		0.288(4)
5(Q)	17.5		0.435(6)
7(Q)	34.9		0.612(5)
2	1.9	0.1295	0.261(6)
3	5.4	0.127	0.305(5)
4	10.2	0.1265	0.380(3)
5	16.4	0.1265	0.474(3)

TABLE II: Data in Fig. 2, $C(N_c)$ at $\sqrt{t}/r_1 = 0.46$. "Q" labels quenched data.

[1] For a review, see R. Sommer, PoS LATTICE **2013**, 015 (2014) [arXiv:1401.3270 [hep-lat]].

[2] R. Sommer, Nucl. Phys. B **411**, 839 (1994). doi:10.1016/0550-3213(94)90473-1 [hep-lat/9310022].

[3] M. Lscher, JHEP **1008**, 071 (2010) Erratum: [JHEP **1403**, 092 (2014)] doi:10.1007/JHEP08(2010)071, 10.1007/JHEP03(2014)092 [arXiv:1006.4518 [hep-lat]].

[4] R. Narayanan and H. Neuberger, JHEP **0603**, 064 (2006) doi:10.1088/1126-6708/2006/03/064 [hep-th/0601210]. M. Luscher, Commun. Math. Phys. **293**, 899 (2010) doi:10.1007/s00220-009-0953-7 [arXiv:0907.5491 [hep-lat]].

[5] O. Bar and M. Golterman, Phys. Rev. D **89**, no. 3, 034505 (2014) Erratum: [Phys. Rev. D **89**, no. 9, 099905 (2014)] doi:10.1103/PhysRevD.89.099905, 10.1103/PhysRevD.89.034505 [arXiv:1312.4999 [hep-lat]].

[6] G. 't Hooft, Nucl. Phys. B **72**, 461 (1974). doi:10.1016/0550-3213(74)90154-0

[7] B. Lucini and M. Panero, Phys. Rept. **526**, 93 (2013) doi:10.1016/j.physrep.2013.01.001 [arXiv:1210.4997 [hep-th]].

[8] T. DeGrand, Phys. Rev. D **86**, 034508 (2012). doi:10.1103/PhysRevD.86.034508 [arXiv:1205.0235 [hep-lat]].

[9] G. S. Bali, F. Bursa, L. Castagnini, S. Collins, L. Del Debbio, B. Lucini and M. Panero, JHEP **1306**, 071 (2013). doi:10.1007/JHEP06(2013)071 [arXiv:1304.4437 [hep-lat]].

[10] T. DeGrand and Y. Liu, Phys. Rev. D **94**, no. 3, 034506 (2016) doi:10.1103/PhysRevD.94.034506 [arXiv:1606.01277 [hep-lat]].

[11] C. W. Bernard *et al.*, Phys. Rev. D **62**, 034503 (2000). doi:10.1103/PhysRevD.62.034503 [hep-lat/0002028].

[12] A. Bazavov *et al.* [MILC Collaboration], Rev. Mod. Phys. **82**, 1349 (2010). doi:10.1103/RevModPhys.82.1349 [arXiv:0903.3598 [hep-lat]].

[13] A. Hasenfratz and F. Knechtli, Phys. Rev. D **64**, 034504 (2001). doi:10.1103/PhysRevD.64.034504 [hep-lat/0103029].

[14] A. Hasenfratz, R. Hoffmann and S. Schaefer, JHEP **0705**, 029 (2007). doi:10.1088/1126-6708/2007/05/029 [hep-lat/0702028].

[15] A. Bazavov *et al.* [MILC Collaboration], Phys. Rev. D **93**, no. 9, 094510 (2016) doi:10.1103/PhysRevD.93.094510 [arXiv:1503.02769 [hep-lat]].

[16] S. Borsanyi *et al.*, JHEP **1209**, 010 (2012) doi:10.1007/JHEP09(2012)010 [arXiv:1203.4469 [hep-lat]].

[17] A. Deuzeman and U. Wenger, PoS LATTICE **2012**, 162 (2012).

[18] R. J. Dowdall, C. T. H. Davies, G. P. Lepage and C. McNeile, Phys. Rev. D **88**, 074504 (2013) doi:10.1103/PhysRevD.88.074504 [arXiv:1303.1670 [hep-lat]].

[19] M. Bruno *et al.* [ALPHA Collaboration], PoS LATTICE **2013**, 321 (2014) [arXiv:1311.5585 [hep-lat]].

[20] A. Bazavov *et al.* [HotQCD Collaboration], Phys. Rev. D **90**, 094503 (2014) doi:10.1103/PhysRevD.90.094503 [arXiv:1407.6387 [hep-lat]].

[21] M. Cé, M. Garca Vera, L. Giusti and S. Schaefer, Phys. Lett. B **762**, 232 (2016) doi:10.1016/j.physletb.2016.09.029 [arXiv:1607.05939 [hep-lat]].

[22] http://www.physics.utah.edu/~detar/milc/